Phosphine-Enhanced Semi-Hydrogenation of Phenylacetylene by Cobalt Phosphide Nano-Urchins

Anthony Ropp, Rémi André, Sophie Carenco

▶ **To cite this version:**

Anthony Ropp, Rémi André, Sophie Carenco. Phosphine-Enhanced Semi-Hydrogenation of Phenylacetylene by Cobalt Phosphide Nano-Urchins. ChemPlusChem, 2023, 88 (11), pp.e202300469. 10.1002/cplu.202300469 . hal-04281515

HAL Id: hal-04281515

https://hal.sorbonne-universite.fr/hal-04281515

Submitted on 13 Nov 2023

HAL is a multi-disciplinary open access archive for the deposit and dissemination of scientific research documents, whether they are published or not. The documents may come from teaching and research institutions in France or abroad, or from public or private research centers.

L'archive ouverte pluridisciplinaire **HAL**, est destinée au dépôt et à la diffusion de documents scientifiques de niveau recherche, publiés ou non, émanant des établissements d'enseignement et de recherche français ou étrangers, des laboratoires publics ou privés.

Phosphine-Enhanced Semi-Hydrogenation of Phenylacetylene by Cobalt Phosphide Nano-Urchins

Mr. Anthony Ropp,[1] Dr. Rémi F. André,[1] Dr. Sophie Carenco,[1,]*

[1] Sorbonne Université, CNRS, Laboratoire de Chimie de la Matière Condensée de Paris (LCMCP), 4 place Jussieu, 75005 Paris, France

E-mail: sophie.carenco@sorbonne-universite.fr

Abstract:

Transition metal phosphides are promising, selective, and air-stable nanocatalysts for hydrogenation reactions. However, they often require fairly high temperatures and H_2 pressures to provide quantitative conversions. This work reports the positive effect of phosphine additives on the activity of cobalt phosphide nano-urchins for the semi-hydrogenation of phenylacetylene. While the nanocatalyst's activity was low under mild conditions (7 bar of H_2, 100 °C), the addition of a catalytic amount of phosphine remarkably increased the conversion, *e.g.*, from 13 % to 98 % in the case of P^nBu_3. The heterogeneous nature of the catalyst was confirmed by negative supernatant activity tests. The catalyst integrity was carefully verified by *post-mortem* analyses (TEM, XPS, and liquid ^{31}P NMR). A stereo-electronic map was proposed to rationalize the activity enhancement provided over a selection of nine phosphines: the strongest effect was observed for low to moderately hindered phosphines, associated with strong electron donor abilities. A threshold in phosphine

stoichiometry was revealed for the enhancement of activity to occur, which was related to the ratio of phosphine to surface cobalt atoms.

Introduction

Transition metal phosphides (TMP) of common transition metals (*e.g.* Mn, Fe, Co, Ni) have emerged as a promising class of catalysts. Because of their high activity and stability, they may be considered very interesting alternatives to the scarce and expensive platinoid catalysts that dominate the field of electrochemical water-splitting.[1–3] As to hydrogenation reactions, TMPs were reported to activate H_2 even under mild conditions and benefit from phosphorus doping in terms of stability and selectivity compared to highly pyrophoric transition metal hydrogenation catalysts like Ni Raney, currently the industrial standard for numerous applications.[3] Indeed, P doping stabilizes nearly zero-valent metallic state in TMP as evidenced by X–Ray Absorption Spectroscopy (XAS).[4] Moreover, the inclusion of phosphide species in a metallic nanoparticle increases the selectivity for alkynes semi-hydrogenation as evidenced for nickel phosphides by Corma *et al*.[5]

Among TMPs, cobalt phosphide catalysts are especially interesting due to their versatility. They were successively tested for the hydrogenations of alkynes (2 bar, 85 °C),[6] nitriles (1 – 40 bar, T > 130 °C),[7,8] carbon monoxide,[9] and as hydrotreating catalysts for the petrochemical industry.[10–13] They finally displayed interesting selectivities for the transformation of furfural to furfuryl alcohol derivatives,[4] nitroarenes to anilines,[14] and levulinic acid to γ-valerolactone.[15,16] We believe that further development of cobalt phosphide catalysts will benefit from a finer control of their shell of organics ligands. Colloidal synthesis proved to be a successful strategy to prepare ligand-covered TMP nanocatalysts with controlled crystallinity and morphology.[17–20] Generally, the influence of native or added ligands on nanocatalysts originates from structural (templating, self-assembly,

orientation) and electronic (Fermi level tuning) effects.[21] However, the effect of ligands, such as phosphines, on catalytic reactions was scarcely investigated for TMP.

These effects may be inferred from studies on metal nanoparticles, which we will discuss now. In most cases, the ligands are responsible for a loss of catalytic activity because of competitive adsorption with substrates.[22,23] In the best cases, they trigger selective reactions by blocking the most reactive sites, which is typically the case for the hydrogenation of alkynes into alkenes. For example, Shevchenko *et al.*[24] showed that tuning the adsorption of amines and phosphines as capping ligands allowed to disfavor alkene adsorption on Pt and $CoPt_3$, resulting in enhanced selectivity for the semi-hydrogenation product. Similar conclusions were drawn for Pd nanocatalyst covered with alkylamines[25] and silica-supported Cu nanoparticles covered with phosphines.[26,27] Only a few studies evidenced a positive influence of ligands on the catalytic activity of nanocatalysts and most of them were provided by the field of semi-heterogeneous Frustrated Lewis Pairs (FLPs) for hydrogenation reactions.[28–30] For instance, while bare gold nanoparticles were not able to catalyze hydrogenation reactions, the addition of piperazine afforded a new pathway for hydrogenation through a concerted hydrogen cleavage between the gold surface and the amine moiety, as evidenced both experimentally and by DFT.[30] More recently, the addition of phosphines on Pd nanoparticles improved both the activity and the selectivity towards the alkene for 1-octyne semi-hydrogenation.[31] The activity enhancements were rationalized thanks to the phosphines' steric and electronic properties, quantified by Tolman parameters.[32] The strongest enhancements were observed for moderately hindered phosphines among the weakest Lewis bases.

To the best of our knowledge, such activity enhancement by ligands was not yet observed for transition metal phosphides nanocatalysts. Because phosphine ligands are tunable in terms of steric and electronic properties and are able to bind to a cobalt phosphide surface, we decided

to investigate this family of Lewis basic molecules. More precisely, our purpose was to evaluate if they could form a semi-heterogeneous FLP with the surface of the cobalt phosphide.

The present work reports the remarkable effect of phosphine on the activity of cobalt phosphide nano-urchins for phenylacetylene semi-hydrogenation. First, the synthesis and detailed characterization of the nano-urchins are described and discussed. Then, their catalytic activity as colloidal suspensions is reported, in the absence or presence of phosphines. While the nanocatalyst's activity was low under mild conditions (7 bar of H_2, 100 °C), the addition of a phosphine significantly increased it. The heterogeneous nature of the catalyst was confirmed by negative supernatant activity tests. The cobalt phosphide nano-urchins as well as the phosphines were mostly not affected by the catalytic reaction as evidenced by Transmission Electron Microscopy (TEM), X-Ray Photoelectron Spectroscopy (XPS), and liquid ^{31}P NMR. A stereo-electronic map was used to compare the phosphine effects, showing that strongly donating phosphines with low to moderate steric hindrance were more favorable. Further experiments indicated a minimum number of phosphine molecules *per* surface cobalt atom was required to trigger the synergetic effect. This enhancement was also observed in several solvents (toluene, THF, acetonitrile).

Results and discussion

Synthesis and characterization of CoP nano-urchins

Cobalt phosphide nano-urchins were synthesized in colloidal suspension at 320 °C by the reduction of $Co(acac)_2$ with oleylamine in the presence of tri-*n*-octylphosphine as a phosphidizing agent (Figure 1A) (see experimental section for details). The formation of nano-urchins with 10 nm-diameter branches was evidenced by TEM. While the urchin morphology was repeatable, the synthesis presented a high batch-to-batch variability as to the

urchin average size, ranging from 200 nm to 1500 nm. As all synthetic parameters, including the heating and stirring rates, were nominally the same, such a variation points out the high sensitivity of the synthesis outcome to little variations in heating or stirring.

This is yet another example of how delicate the production of phase- and morphology-controlled nanoparticles can be.[33] Potential consequences are slight variations of the specific surface and the precise nature of surface sites.

Local phosphorus/cobalt ratios, determined by Energy Dispersive X-Ray Spectroscopy in Scanning Transmission Electron Microscopy (STEM-EDX) on several urchin cores and branches, evidenced that the latter were slightly phosphorus-richer (P/Co of 1.4 *vs.* 1.2 for the cores, see SI section 2). One should note the measurements aggregated both the contributions of alkylphosphine surface ligands and the phosphorus incorporated in the crystal structure.

Powder X-Ray Diffraction (XRD) confirmed the formation of the orthorhombic CoP phase (ICDD N°00-029-0497) as the major phase. Orthorhombic Co_2P (ICDD N°04-007-1524) traces were nonetheless detected as a minor phase, at various levels depending on the samples (Figure S1). While the urchins' branches account for most of the sample's surface, XRD measurements were representative of the larger crystalline domains, *i.e.*, likely urchins' cores.

High Resolution TEM (HRTEM) confirmed the CoP crystal structure of the nano-urchins' branches, with an indexation of the electron diffraction pattern in agreement with XRD (Figure 1D and E). All observed distances were indeed compatible with branches exposing CoP. Nevertheless, the proximity of plane distances between Co_2P and CoP made some of the plane indexation ambivalent (see SI section 2).

Overall, Co_2P was present in variable amounts in the different batches, but it was always a minor phase that we located in the core of the urchins. Thus, only CoP was likely involved in the catalytic process and the catalyst will be denoted as "CoP nano-urchins" in the following, for the sake of simplicity.

The use of 2 mmol of $Co(acac)_2$ only afforded 200 mg of CoP nano-urchins, corresponding to a quantitative yield. As will be showed in the next section, this single batch allowed us to unravel the positive effect of phosphine addition on the catalytic reaction. However, a detailed investigation of the catalytic properties required larger amounts of materials. Upscaling attempts with 6 mmol of $Co(acac)_2$ also yielded in CoP nano-urchins but a large number of rods, nanoparticles and hollow nanoparticles (2 – 20 nm) where systematically obtained and could not be separated. The upscaling failure was attributed to the high sensitivity of the synthesis to the heating rate, stirring and glassware dimensions, which cannot be kept rigorously identical through upscaling. This is unfortunately a problem often encountered when dealing with nanocatalysts synthesis.[35] In such situation, high-throughput techniques[36] may be required to decipher which parameter is critical. However, this was out of the scope of our article, which is focused on the positive effect of phosphine on the hydrogenation activity of these materials.

Considering that each batch already presented a distribution of morphologies and Co_2P impurity, we argued that mixing several batches presenting a phosphine effect would improve the consistency of the following catalytic study.

Therefore, seven CoP nano-urchin batches were mixed, and washed altogether one more time with hexanes and ethanol to homogenize the material's surface state. TEM and XRD pattern of the resulting catalyst, presented in Figure 1 and Figure S6, were consistent with the urchin size polydispersity and Co_2P impurity level observed on average in the separated batches (see SI, section 2).

Overall, the catalyst was composed of nano-urchins, with diameters ranging from 200 to 1500 nm, and consisting of CoP and Co_2P as the major and minor phases, respectively. The average Co/P ratio of 1.2, as measured by SEM-EDX on a 80 µm x 60 µm region, is coherent with such a phase distribution.

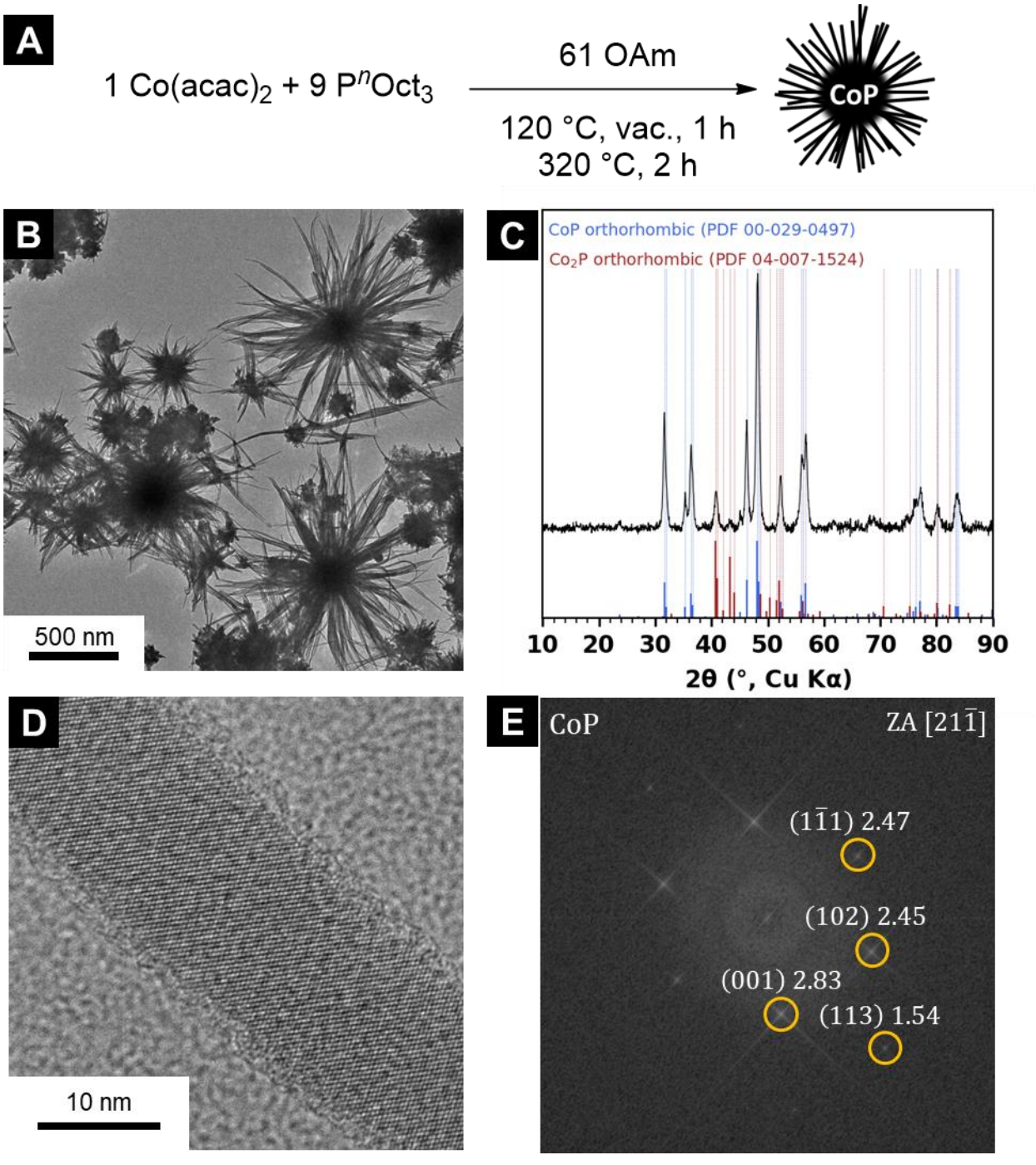

Figure 1. (A) One-pot colloidal synthesis of cobalt phosphide nano-urchins, (B) TEM, (C) XRD of cobalt phosphide nano-urchins batch used for catalysis. (D) Representative HRTEM of cobalt phosphide nano-urchins and (E) plane indexation corresponding to orthorhombic CoP (ZA: zone axis, orange circles are guide to the eye and distances are given in Å).

The chemical nature of cobalt and phosphorus atoms at the extreme surface of the catalyst was probed by XPS. The Co 2p and P 2p regions were analyzed following the methodology of

our previous works (fitting parameters given in SI, section 1).[35,36],[37] Although the Co 2p region was fitted with three components (metallic cobalt, CoO, and Co_3O_4),[37] the metallic cobalt component still accounted for all the signal (binding energy, B.E., 777.8 – 778.1 eV) (Figure S7). The P 2p region was deconvoluted in three doublets with a spin-orbit splitting of 0.85 eV. The main component consisted of reduced P species (129.1 – 129.4 eV, dark blue) at a B.E. lower than elemental P (130.0 eV), as expected for metal phosphides.[38] Two oxidized P species were also detected: P^{III} (130.2 – 131.0 eV, blue), attributed to TOP bound to the surface, and P^{V} (132.7 – 133.0 eV, light blue), attributed to phosphate or tri-*n*-octylphosphine oxide (TOPO), originating from the oxidation of TOP.[38] Overall, the XPS data were consistent with a material presenting a CoP surface surrounded by organic ligands that remained from the synthesis.

Semi-hydrogenation of phenylacetylene enhanced by phosphines

Catalytic reaction with P^nBu_3

CoP nano-urchins were tested as catalysts for the semi-hydrogenation of phenylacetylene as a model compound, with phosphines as molecular additives. A typical experiment was carried out on 1 mmol of phenylacetylene in 2 mL toluene, in mild conditions, *i.e.*, under 7 bar H_2 at 100 °C (see experimental section). The catalytic activity was assessed by determining the conversion (C) of phenylacetylene and the selectivity toward styrene (SS).

The use of CoP nano-urchins (20 mol% [Co], mixed batch) in the absence of phosphine led to a good selectivity (95 %), but a low conversion (13 %) (Table 1 *entry* 0). Interestingly, when P^nBu_3 (0.1 equiv. *vs.* phenylacetylene, $[P^nBu_3]$ = 0.047 mol/L) was added, the conversion became almost quantitative (98 %) with only a slight decrease of selectivity (84 %) (Table 1 *entry* 2). This positive effect of the phosphine on the catalytic process triggered our interest. This effect was also observed on single batches (Table S3) but we preferred to further employ

the mixed batch for the consistency of the following catalytic study that required large amount of materials.

Post-mortem analysis

Firstly, we confirmed that the catalysis was not due to homogeneous species and that the strong activity enhancement was due to the nano-urchins associated with the phosphine by testing the supernatant activity, following a procedure developed in earlier works.[5,39–41] After the reaction, the reaction mixture was centrifuged, and the supernatant was collected and refilled with fresh phenylacetylene (Scheme S1). No further conversion was detected, excluding the formation of catalytically active leached cobalt species.

Furthermore, the recycled CoP nano-urchins were washed three times under inert atmosphere with toluene only and tested for the same reaction, alone or in combination with P^nBu_3 (Scheme S1). Without adding fresh P^nBu_3, the recycled CoP nano-urchins provided a conversion of 42 %, intermediate between that of fresh CoP nano-urchins in combination with P^nBu_3 (98 %) and that of fresh CoP nano-urchins never exposed to P^nBu_3 (13 %). This enhancement of the catalytic activity *vs.* the later sample could be explained by the effect of residual P^nBu_3 adsorbed on the surface, or by the removal of ligands blocking the access to active surface sites during the washing step.

Besides, when 0.1 equiv. of fresh P^nBu_3 was added to the recycled CoP nano-urchins, a complete conversion of phenylacetylene was again observed (Scheme S1). These experiments first confirmed the heterogeneous nature of the catalyst and then underlined the robustness of the enhancement effect with a catalytic quantity of P^nBu_3 even after a recycling test.

Moreover, TEM of the spent catalyst evidenced the retention of the urchin-like morphology, without the formation of small nanoparticles that would have indicated metal leaching and/or nano-urchin restructuration (Figure S10). XPS of the *post-mortem* CoP nano-urchins did not

display any difference in the Co 2p and P 2p regions (Figure S11), suggesting the chemical nature of the surface was unaffected by the catalytic reaction.

The reaction mixture was finally investigated by ^{31}P NMR, under inert conditions to mitigate the oxidation of the phosphine. It should be noted that P^{n}Bu$_3$ was introduced in excess *vs.* the number of available cobalt surface sites. It was thus expected that most of the phosphine molecules are present as free species in the solution during the catalytic reaction. At the end of the reaction, P^{n}Bu$_3$ remained the major observed species (δ = - 32.2 ppm, > 80 %, Figure S12), confirming that most of the P^{n}Bu$_3$ molecules were preserved during the catalytic reaction.

Phosphine screening

In view of the above, the phosphine molecules are apparently involved in a catalytic site at the surface of the urchin, acting either as a Lewis base and/or as a coordinating ligand. To better understand its role, the phosphine steric and electronic properties were varied by changing the nature of its substituents, including various alkyl- and aryl- groups (Table 1).

Styrene selectivity remained high for all tested phosphines (84-100 %), therefore, the following discussion is mainly focused on the conversion. Substituting the linear *n*-butyl group with bulkier *iso*-butyl groups strongly decreased the conversion (20 %), and the activity of CoP nano-urchins was no longer enhanced by P^{t}Bu$_3$ (Table 1, *entries* 3 – 4). P^{n}Oct$_3$ showed an activity enhancement close to that of P^{n}Bu$_3$ (96 %), while PMe$_3$ was less efficient (48 %) (Table 1, *entries* 5 – 6). Substituting phenyl groups with methyl ones further decreased the extent of the activity enhancement as PPhMe$_2$ led to a conversion of 24 % and PPh$_2$PMe and PPh$_3$ did not lead to any measurable improvement of the activity of the CoP nano-urchins (Table 1, *entries* 6 – 9). Finally, PCy$_3$, as a cycloalkyl substituted phosphine, appeared as the third-best phosphine with a conversion of 68 %.

Following a methodology presented in an earlier work,[42] the influence of the phosphine's substituents was rationalized *via* a stereo-electronic map (Figure 2) representing the phenylacetylene conversion on a two-dimensional space based on the phosphine Tolman Electronic Parameter (TEP)[32] and a steric hindrance parameter. The reliability of the Tolman cone angle, determined from nickel-phosphine complexes and generally used as a steric hindrance parameter, has been recently questioned when considering interactions with nanoparticle surfaces. New evaluations of its values, as well as new metrics, were proposed in the recent literature.[43,44] We thus selected a free ligand descriptor, He_8_steric, which purely accounts for the steric hindrance, quantified by the interaction energy of the phosphine with a ring of eight Helium atoms mimicking *cis* coordinated groups in an octahedral environment.[43] The stereo-electronic map (Figure 2) reveals that the phosphine enhancement effect is the most pronounced for the strongest bases (TEP < 2060 cm^{-1}) that have a moderate steric hindrance.

Table 1. Phosphine screening (20 mol% CoP, 0.1 equiv. PR_3, 100 °C, 23 h). Phenylacetylene conversion and styrene selectivity were computed as described in the SI based on NMR integrations.

Entry	Catalyst	Phosphine	PhCCH conversion (%)	Styrene selectivity (%)
0	CoP	–	13	95
1	–	P^nBu_3	0	–
2	CoP	P^nBu_3	98	84
3	CoP	P^iBu_3	20	92
4	CoP	P^tBu_3	14	100
5	CoP	P^nOct_3	96	89
6	CoP	PMe_3	48	94
7	CoP	$PPhMe_2$	24	90
8	CoP	PPh_2Me	9	89
9	CoP	PPh_3	15	92
10	CoP	PCy_3	68	90

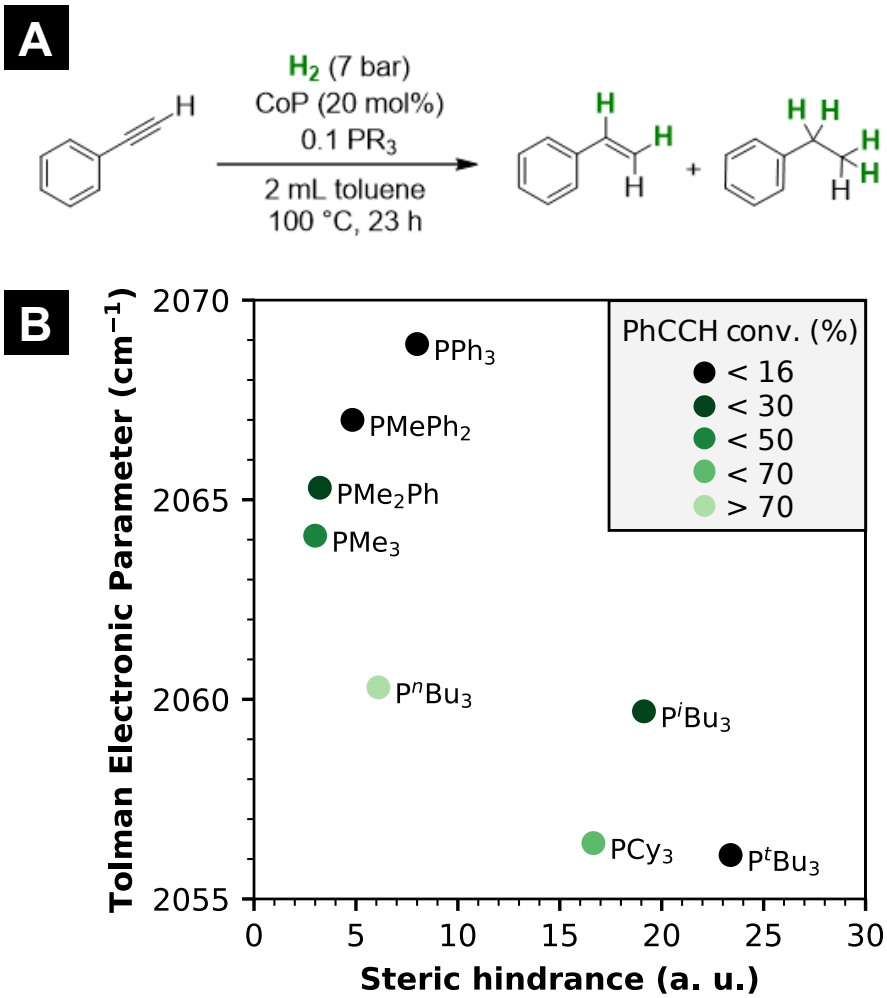

Figure 2. (A) Catalytic reaction and operating conditions. (B) Stereo-electronic map displaying phenylacetylene conversion for all the phosphines tested (alkyl- and arylphosphines). The color code for the conversion of phenylacetylene is indicated in the top right corner of the figure.

Activity threshold in relation to the phosphine amount

The next question was to investigate how many phosphine molecules are necessary for the activity enhancement to occur. For this purpose, P^nBu_3 was selected as a model phosphine whose stoichiometry was varied from 0.05 equiv. to 1 equiv. (Figure 3 and Table S4). The CoP catalytic charge was decreased to 10 mol% to be able to compare the activity at lower conversions, not limited by the availability of phenylacetylene. No enhancement was detected at low P^nBu_3 stoichiometry (< 0.05 equiv.). A significant enhancement was observed at

0.10 equiv. (0.05 mol/L) for which two nominally identical experiments led to very different conversions (6 % and 97 %). This suggested that the threshold value was close to 0.1 equiv. and within the margin of error due to the use of the micropipette for adding the phosphine. At higher stoichiometries (> 0.20), the conversion was high (> 80 %) but softly declined. The increasing phosphine concentration may favor parasitic interactions with phenylacetylene or poison cobalt phosphide active surface sites due to too frequent adsorption of the phosphine molecules on the surface.[22,45]

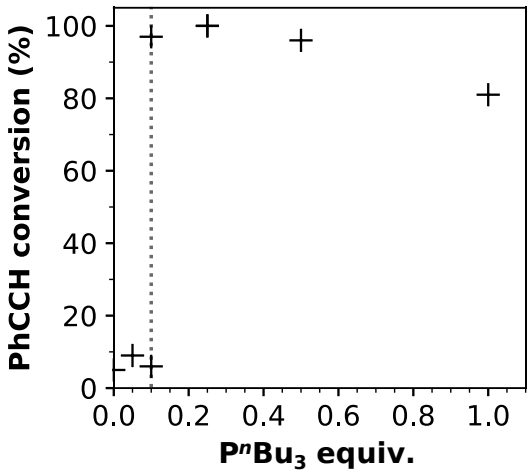

Figure 3. Threshold of CoP catalytic activity with P^{n}Bu$_3$ stoichiometry *vs.* phenylacetylene (10 mol% CoP, 100 °C, 23 h). The dotted line is a guide to the eye, indicating the position of the threshold.

At this point, the enhancement effect of the phosphine on the CoP nano-urchin surface was demonstrated, and it was clear that a minimal amount of phosphine was required for the effect to take place. These ligands come in a large excess compared with those present at the surface of the nano-urchins at the end of their synthesis, which were investigated next.

Activity enhancement by addition of tri-n-octylphosphine and oleylamine

After the colloidal synthesis of CoP nano-urchins, some organic ligands remained from the synthesis or as a result of side-reaction during the synthesis.[46,47] These ligands were beneficial for the dispersibility and colloidal stability during catalysis although their limited amount is well below the threshold identified above. Thus, we decided to extend the scope of the tested additives to molecules that were suspected to already cover the native surface in limited amount (ligands from the synthesis or degradation products). Indeed, as CoP nano-urchins were washed in air, various amounts of oleylamine (primary long-chain amine solvent and reducing agent) as well as tri-*n*-octylphosphine and tri-*n*-octylphosphine oxide remained at their surface.[46,48]

As aforementioned, the addition of 0.10 equiv. of P^nOct_3 led to a similar conversion enhancement as P^nBu_3, which can be explained by the similarities in structure and basicity (Table S5, *entry* 1b). Besides, $O=P^nOct_3$ addition did not enhance the phenylacetylene conversion. More surprisingly, oleylamine addition led to a conversion increase (from 7 % to 51 %, Table S5, *entry* 2c), without significant hydrogenation of its internal double bond as proved by ^1H NMR (Figure S13). Such a result clearly demonstrates the synergetic effect is not limited to phosphine molecules and may be extended to amines, underlining the probable role of the Lewis base/coordination capacity of the co-catalyst. The positive impact of these ligands partially explains the activity variability between catalysts batches as their amount may vary slightly at the end of the washing procedure. In the next section, we investigated another aspect, dealing with the interaction of the phosphine with H_2.

Attempts to trap a reaction intermediate involving the phosphine

Given the heterogeneous nature of the catalysis, associated with the critical influence of the phosphine substituents, the involvement of the phosphine in a heterolytic cleavage of

hydrogen, yielding a surface hydride and a protonated phosphine, was envisioned. Such a mechanism, inspired by the chemistry of Frustrated Lewis Pairs, has already been evidenced for hydrogen splitting between gold surfaces and N-bases (imines, diamines).[29,49]

Thus, we first attempted to trap a potential phosphonium species ($HP^nBu_3^+$) using $NaBF_4$ as a BF_4^- counter-anion source. However, the corresponding phosphonium salt ($HP^nBu_3^+/BF_4^-$) was poorly soluble in toluene while it was soluble in more polar solvent such as tetrahydrofuran (THF) or acetonitrile. Therefore, the influence of the solvent polarity on the phosphine effect was studied with these two solvents presenting similar H_2 solubilities as toluene (Table S7).[50] Due to practical limitations, this complementary study was performed on a single batch that was thoroughly characterized by XRD and TEM, and the data are presented in the supplementary information file (Figure S14). As variations in conversion levels and/or threshold values are expected due to slightly different surface state and environment, data were interpreted within this sub-study. In the absence of phosphine, the conversion was above 60 % in acetonitrile, more polar than toluene and THF. The enhancement due to the phosphine addition was almost insensitive to the solvent polarity, with conversions of respectively 94 % and 93 % in THF and acetonitrile (*vs.* 89 % in toluene). The attempt to trap a reaction intermediate was therefore conducted in acetonitrile that afforded a good solubility of the phosphonium, with CoP nano-urchins (mixed batch). After 16h under 7 bar H_2 at 100 °C, only P^nBu_3 and oxidation products were detected by ^{31}P NMR, but no phosphonium species (Figure S15).

The direct use of $HP^nBu_3BF_4$ (0.35 equiv.) as an additive in toluene led to a conversion of 16 %, with a selectivity of 93 %. Thus, no significant increase in conversion was observed compared to CoP alone, evidencing the failure of the phosphonium to enter a catalytic cycle in these conditions. However, according to ^{31}P NMR, 17 % of the phosphonium was deprotonated during the reaction, suggesting that it reacted with the CoP surface (Figure S16).

Further investigations would be required to clarify the possible three-body interactions between the phosphine, H_2 and the surface.

Discussion

In the results presented above, several key points were identified for the activity enhancement of TMP nanocatalysts by phosphines. Regarding the CoP nano-urchins synthesis, the presence of a Co_2P impurity could be explained by a migration mechanism occurring when inserting light elements into a metallic matrix.[51] This mechanism is typically involved in the partial phosphidizing of metallic nanocrystals while the core remains metallic or in a phosphorus poorer metal phosphide phase.[51] Because urchin's branches were richer in phosphorus than their cores according to STEM-EDX measurements, we suggest that urchins nucleated as Co(0) or Co_2P while CoP was obtained by further insertion and migration of phosphorus liberated by the degradation of tri-*n*-octylphosphine on the surface.

Regarding the catalysis experiments, although phosphine addition would generally be expected to negatively impact the catalyst activity due to competition with the adsorption of reagents, we rather demonstrated here a strong activity enhancement by selected phosphines.

Firstly, phenylacetylene semi-hydrogenation by cobalt phosphide nano-urchins was robustly enhanced by the addition of a well-chosen phosphine despite batch-to-batch variability (in urchin size and level of Co_2P impurity). While the phosphine enhancement effect was robust between batches, the catalytic activities varied strongly. This could be first explained by changes in specific surface area due to variations in nano-urchins' diameters (200 – 1500 nm) and variabilities in Co_2P impurity level, although our study pointed out that mostly CoP surfaces were exposed (Figure 4A). Then, the addition of tri-*n*-octylphosphine and oleylamine was proven to enhance the hydrogenation catalytic activity: variable residual amounts of ligands after the washing steps could explain the batch-to-batch variation of catalytic activity.

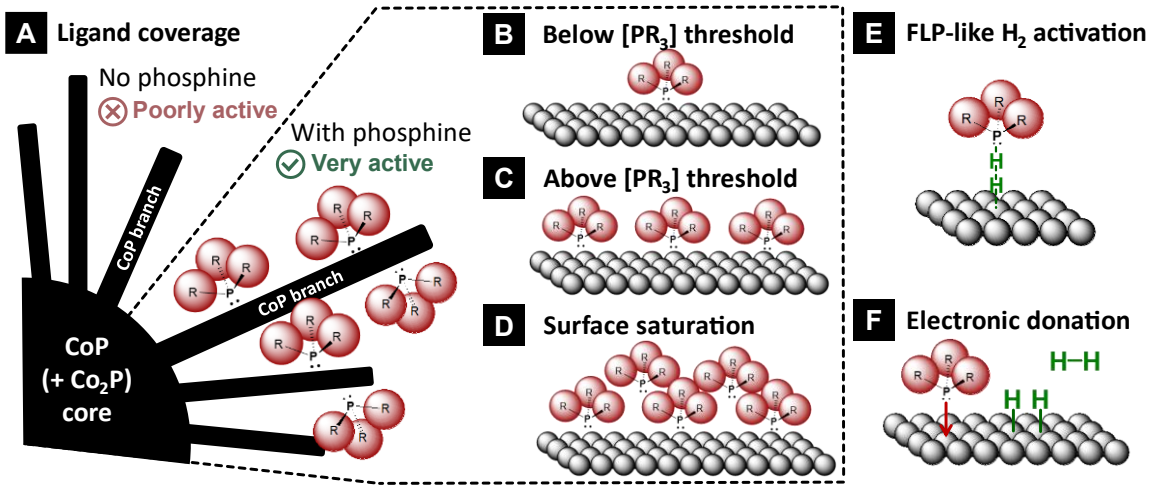

Figure 4. (A) Schematic representations of the nanocatalyst exposing CoP branches, (B)-(D) the surface at various phosphine coverage ratios and schemes of the mechanism proposal: (E) concerted H_2 activation between the CoP surface and the phosphine and/or (F) electronic donation effect of the phosphine.

Secondly, we evidenced that specific conditions were required to observe an activity enhancement by the addition of a phosphine. Particularly, the activity threshold observed suggested that a minimal coverage of the surface by the added phosphine was required (Figure 4B-D). This threshold could also be interpreted as the requirement of a minimal phosphine concentration that must be reached to displace the adsorption equilibrium of ligands present after the synthesis (native ligands). The corresponding threshold concentration likely depends on the relative adsorption strength of the phosphine and the native ligands.

According to a geometrical model, the apparent number of phosphine molecules *per* surface metal atom was evaluated for this work and for two other studies where a similar phosphine-related activity enhancement was observed (see SI, section 11). The activity threshold occurred when introducing roughly ten phosphine molecules *per* surface cobalt atom. Reported phosphine activity enhancements also required a minimal PR_3:surface metal ratio, which was estimated to be just above 1. Phosphine-assisted benzaldehyde hydrosilylation by NiCo nanoparticles was observed from 1.6 PR_3:surface metal atom.[40] Similarly, 1-octyne

hydrogenation by Pd nanoparticles was strongly enhanced by the addition of 1.4 PPh_3 per surface Pd.[31] In all cases, a small excess of phosphine seems to be required. Excess phosphine was however not targeted for the two studies because it may decrease the catalytic activity by blocking the substrate's adsorption sites or even lead to secondary products resulting from the interaction with the substrate.

Besides, our study demonstrated that the activity enhancement was the strongest for the best electron-donating phosphines with a moderate steric hindrance. Too bulky additives could not approach the surface due to the presence of native ligands with long alkyl chains which would hinder the approach of the substrate. Their strong electron-donation abilities could relate to their propensity to bind the metal surface and to displace native ligands.

Inspired by Frustrated Lewis Pair catalysis, we wondered whether the phosphine would be involved in a concerted hydrogen cleavage with the surface (Figure 4E). In such framework, the colloidal suspension of cobalt phosphide and the soluble phosphine ligands would be forming together a semi-heterogeneous FLP. To be more precise, we could consider this species to be a NanoFLP,[40] meaning a FLP at the surface of a nanoparticle in a colloidal suspension. A direct proof of the concerted cleavage of H_2 would have been to detect the formation of the resulting phosphonium species. Experimental evidence of a similar concerted action was provided by Rossi *et al.* studying piperazine-assisted hydrogenation with gold nanoparticles. They were able to observe by *in situ* ^{1}H NMR the corresponding ammonium species.[30] Unfortunately, we did not manage to detect a phosphonium in the present study, either because it did not form, or because it was not soluble and concentrated enough to be detected by ^{31}P NMR. Thus, while a concerted hydrogen activation cannot be ruled out at this stage, it is also possible that the phosphine electronic donation to the surface was enough to boost its catalytic properties (Figure 4F), which was supported by the stereo-electronic map.

Conclusion

In conclusion, we reported the colloidal synthesis of cobalt phosphide nano-urchins. The experimental variability of the synthesis outcome in terms of cobalt phosphide phase and urchin size proved to be significant but manageable for our catalytic study. An HRTEM analysis concluded that the branches, which represented most of the surface of the samples were crystalline CoP. The nanocatalyst was poorly active for phenylacetylene semi-hydrogenation in mild conditions (7 bar H_2, 100 °C) but well-chosen phosphines strongly enhanced its activity in the temperature range 60 – 100 °C.

A stereo-electronic map was proposed to rationalize the activity enhancement: the strongest effect was observed for low to moderately hindered phosphines with the strongest electron donor abilities. Decreasing the amount of added phosphine revealed an activity threshold, suggesting that a minimal amount of phosphine was required for the activity to be enhanced. Such a threshold would lead us to reconsider poorly active nanocatalysts and study their activity under milder conditions. Although preliminary mechanistic studies were not conclusive, the stereo-electronic map suggests that the phosphine's electronic donation to the surface is of key importance.

Further work is ongoing to better understand the enhancement effect observed with CoP but also other hydrogenation transition metal nanocatalysts. In order to generalize the positive effect of selected phosphines to other metal phosphides (*e.g.* Ni_2P) and transition metals (*e.g.* nickel), complementary studies are on-going and will be reported in due time. Further spectroscopic studies as well as computational modeling would be helpful to provide a deeper understanding of the dynamics of the phosphine ligands on the nanocatalyst's surface.

Experimental Section

Reagents and general information

Oleylamine (OAm; 98 %), cobalt(II) acetylacetonate ($Co(acac)_2$; >99 %, anhydrous), toluene (99.8 %, anhydrous), acetonitrile (MeCN; 99.8 %, anhydrous), tetrahydrofuran (THF; 99.99 %, anhydrous, inhibitor free), trimethylphosphine (PMe_3; 99 %), dimethylphenylphosphine (PMe_2Ph; 99 %), diphenylmethylphosphine ($PMePh_2$; 99 %), triphenylphosphine (PPh_3; 99 %), tri-*n*-octylphosphine oxide ($O=P^nBu_3$; 99 %), tri-*t*-butylphosphine (P^tBu_3; 98 %) and phenylacetylene (PhCCH; 98%) were purchased from Sigma-Aldrich. Tri-*n*-octylphosphine (TOP; 97 %), tri-*n*-butylphosphine (P^nBu_3; 99 %), tri-*i*-butylphosphine (P^iBu_3; <93 %), tricyclohexylphosphine (PCy_3; 97 %), tri-*n*-butylphosphonium tetrafluoroborate ($HP^nBu_3BF_4$; 97 %) were purchased from Strem Chemical and stored in a glovebox. Ethanol (EtOH; 96 %) was purchased from VWR.

Hydrogen gas bottles were purchased from AirLiquide (N55, 150 bar, 140 L, $H_2 \geq 99.99995$ %). Deuterated chloroform ($CDCl_3$; 99.5 %), toluene (tol-d8; 99.5 %) and acetonitrile (MeCN-d3; 99.8 %) were purchased from Euriso-top. All chemicals described above were used without further purification. Glassware was kept in an oven at 120 °C prior to utilization.

Synthesis of CoP nano-urchins

The synthesis was adapted from a reported procedure, for the formation of CoP spherical nanoparticles (20 nm), using a one-pot colloidal synthesis.[52] In our hands, the following protocol reproducibly produced CoP nano-urchins.

A three-neck round bottom flask equipped with a thermocouple (inside a glass insert) was charged with the oleylamine (61 equiv., 40 mL, 122 mmol). The flask was connected to a Schlenck line with a Nalgene tube and through a vertical condenser (used to avoid spilling of

the oleylamine in the Nalgene tube). Oleylamine was degassed by three brief vacuum/N_2 cycles at 50 °C. $Co(acac)_2$ (1 equiv., 2 mmol, 514 mg) was collected in the glovebox and added under a nitrogen flow to the flask containing oleylamine. The mixture was then heated up to 120 °C under dynamic vacuum for 1 h to remove water and other low-boiling point impurities. Subsequently, tri-*n*-octylphosphine (9 equiv., 8 mL) was added under a nitrogen flow and the carmine red mixture was heated up to 320 °C for 2 h. The mixture's color shifted to deep green at 220 °C and became black at 320 °C. After 2 hours, the mixture was cooled down to room temperature. The mixture was transferred to two 50 mL centrifugation tubes with a small amount of hexane (30 mL) and 10 mL of ethanol was added to each tube to foster aggregation and sedimentation of the nano-urchins. The mixture was centrifugated at 9000 rpm for 5 min. Then, CoP nano-urchins were washed three times at 9000 rpm for 5 min. Between each centrifugation step the nanoparticles were redispersed in hexane (10 mL) and ethanol (30 mL) was then added to foster aggregation. After drying overnight in air at room temperature, a black powder of CoP nano-urchins was obtained and carefully ground into a fine powder. 200 mg of powder were collected. An approximative yield *vs.* CoP can be calculated by neglecting the weight of remaining surface ligands: 110 %.

Hydrogenation of phenylacetylene

In the glovebox, a 50 mL Büchi glass batch reactor was charged with phenylacetylene (1 equiv., 1 mmol, 110 µL), a catalytic amount of CoP nano-urchins (20 mol%, 18 mg, based on CoP stoichiometry), tri-*n*-butylphosphine (0.1 equiv., 25 µL) and toluene (2 mL). The autoclave was then charged with 7 bar H_2 and heated at 100 °C for 23 h. After cooling down to r.t., the mixture was filtrated. NMR tubes were prepared by diluting a drop of the reaction mixture in $CDCl_3$.

Supporting Information

Additional experimental details and methods, characterization of CoP nano-urchins (XRD, TEM, HRTEM, STEM-EDX, XPS), *post-mortem* analyses (XPS, TEM, $^{31}P\{^{1}H\}$ NMR) and estimations of the quantity of dissolved hydrogen and of ligand *vs.* surface metal ratio.

Acknowledgments

This project has received funding from the European Research Council (ERC) under the European Union's Horizon 2020 research and innovation program (grant agreement No 758480). Sorbonne Université and CNRS are acknowledged for support. Antoine Miche and Sandra Casale (Sorbonne Université, CNRS, Fédération de Chimie et Matériaux de Paris-Centre, LRS) are respectively acknowledged for the XPS measurements and STEM-EDX and HRTEM acquisitions.

Keywords

cobalt phosphide, hydrogenation, ligand effects, nanocatalysis, nanostructures

Author contributions

A. R. conducted the syntheses, the characterizations, and the catalysis experiments. R.F.A. replicated the syntheses and participated in the condition investigations. A. R. and S. C. conceived the project and co-wrote the manuscript, S. C. spearheading it. All authors approved the final version of the manuscript.

References

[1] Y. Pan, Y. Lin, Y. Chen, Y. Liu, C. Liu, *J. Mater. Chem. A* **2016**, *4*, 4745–4754.

[2] J. F. Callejas, C. G. Read, E. J. Popczun, J. M. McEnaney, R. E. Schaak, *Chem. Mater.* **2015**, *27*, 3769–3774.

[3] J. C. Kim, D. W. Kim, *Int. J. Energy Res.* **2022**, *46*, 13035–13043.

[4] H. Ishikawa, M. Sheng, A. Nakata, K. Nakajima, S. Yamazoe, J. Yamasaki, S. Yamaguchi, T. Mizugaki, T. Mitsudome, *ACS Catal.* **2021**, *11*, 750–757.

[5] S. Carenco, A. Leyva-Pérez, P. Concepción, C. Boissière, N. Mézailles, C. Sanchez, A. Corma, *Nano Today* **2012**, *7*, 21–28.

[6] M. F. Delley, Z. Wu, M. E. Mundy, D. Ung, B. M. Cossairt, H. Wang, J. M. Mayer, *J. Am. Chem. Soc.* **2019**, *141*, 15390–15402.

[7] T. Mitsudome, M. Sheng, A. Nakata, J. Yamasaki, T. Mizugaki, K. Jitsukawa, *Chem. Sci.* **2020**, *11*, 6682–6689.

[8] M. Sheng, S. Yamaguchi, A. Nakata, S. Yamazoe, K. Nakajima, J. Yamasaki, T. Mizugaki, T. Mitsudome, *ACS Sustain. Chem. Eng.* **2021**, *9*, 11238–11246.

[9] X. Song, Y. Ding, W. Chen, W. Dong, Y. Pei, J. Zang, L. Yan, Y. Lu, *Energy and Fuels* **2012**, *26*, 6559–6566.

[10] S. T. Oyama, *J. Catal.* **2003**, *216*, 343–352.

[11] J. A. Cecilia, A. Infantes-Molina, E. Rodríguez-Castellón, A. Jiménez-López, *Appl. Catal. B Environ.* **2009**, *92*, 100–113.

[12] A. Berenguer, T. M. Sankaranarayanan, G. Gómez, I. Moreno, J. M. Coronado, P. Pizarro, D. P. Serrano, *Green Chem.* **2016**, *18*, 1938–1951.

[13] X. Zhou, X. Li, R. Prins, J. Lv, A. Wang, Q. Sheng, *J. Catal.* **2021**, *394*, 167–180.

[14] S. Yang, L. Peng, E. Oveisi, S. Bulut, D. T. Sun, M. Asgari, O. Trukhina, W. L. Queen, *Chem. - A Eur. J.* **2018**, *24*, 4234–4238.

[15] H. J. Feng, X. C. Li, H. Qian, Y. F. Zhang, D. H. Zhang, D. Zhao, S. G. Hong, N. Zhang, *Green Chem.* **2019**, *21*, 1743–1756.

[16] R. Q. Raguindin, B. Z. Desalegn, M. N. Gebresillase, J. G. Seo, *Renew. Energy* **2022**, *191*, 763–774.

[17] M. R. Buck, R. E. Schaak, *Angew. Chemie - Int. Ed.* **2013**, *52*, 6154–6178.

[18] M. E. Mundy, D. Ung, N. L. Lai, E. P. Jahrman, G. T. Seidler, B. M. Cossairt, *Chem. Mater.* **2018**, *30*, 5373–5379.

[19] D. R. Liyanage, S. J. Danforth, Y. Liu, M. E. Bussell, S. L. Brock, *Chem. Mater.* **2015**, *27*, 4349–4357.

[20] Q. Liang, K. Huang, X. Wu, X. Wang, W. Ma, S. Feng, *RSC Adv.* **2017**, *7*, 7906–7913.

[21] D. Wu, D. Han, W. Zhou, S. Streiff, A. Y. Khodakov, V. V. Ordomsky, *Catal. Rev. - Sci. Eng.* **2022**, DOI 10.1080/01614940.2022.2079809.

[22] L. Lu, S. Zou, B. Fang, **2021**, DOI 10.1021/acscatal.1c00903.

[23] S. Kunz, *Top. Catal.* **2016**, *59*, 1671–1685.

[24] S. G. Kwon, G. Krylova, A. Sumer, M. M. Schwartz, E. E. Bunel, C. L. Marshall, S.

Chattopadhyay, B. Lee, J. Jellinek, E. V. Shevchenko, *Nano Lett.* **2012**, *12*, 5382–5388.

[25] Q. Luo, Z. Wang, Y. Chen, S. Mao, K. Wu, K. Zhang, Q. Li, G. Lv, G. Huang, H. Li, Y. Wang, *ACS Appl. Mater. Interfaces* **2021**, *13*, 31775–31784.

[26] A. Fedorov, H. J. Liu, H. K. Lo, C. Copéret, *J. Am. Chem. Soc.* **2016**, *138*, 16502–16507.

[27] N. Kaeffer, K. Larmier, A. Fedorov, C. Copéret, *J. Catal.* **2018**, *364*, 437–445.

[28] Y. Ma, S. Zhang, C.-R. Chang, Z.-Q. Huang, J. C. Ho, Y. Qu, *Chem. Soc. Rev.* **2018**, *47*, 5541–5553.

[29] G. Lu, P. Zhang, D. Sun, L. Wang, K. Zhou, Z.-X. Wang, G.-C. Guo, *Chem. Sci.* **2014**, *5*, 1082.

[30] J. L. Fiorio, E. C. M. Barbosa, D. K. Kikuchi, P. H. C. Camargo, M. Rudolph, A. S. K. Hashmi, L. M. Rossi, *Catal. Sci. Technol.* **2020**, *10*, 1996–2003.

[31] L. Staiger, T. Kratky, S. Günther, O. Tomanek, R. Zbořil, R. W. Fischer, R. A. Fischer, M. Cokoja, *ChemCatChem* **2021**, *13*, 227–234.

[32] C. A. Tolman, *Chem. Rev.* **1977**, *77*, 313–348.

[33] A. Palazzolo, C. Poucin, A. P. Freitas, A. Ropp, C. Bouillet, O. Ersen, S. Carenco, *Nanoscale* **2022**, DOI 10.1039/D2NR00917J.

[34] E. M. Chan, C. Xu, A. W. Mao, G. Han, J. S. Owen, B. E. Cohen, D. J. Milliron, *Nano Lett.* **2010**, *10*, 1874–1885.

[35] S. Carenco, C.-H. Wu, A. Shavorskiy, S. Alayoglu, G. A. Somorjai, H. Bluhm, M. Salmeron, *Small* **2015**, *11*, 3045–3053.

[36] J. Kolny-Olesiak, *Zeitschrift fur Naturforsch. - Sect. A J. Phys. Sci.* **2019**, *74*, 709–719.

[37] M. C. Biesinger, B. P. Payne, A. P. Grosvenor, L. W. M. Lau, A. R. Gerson, R. S. C. Smart, *Appl. Surf. Sci.* **2011**, *257*, 2717–2730.

[38] S. Carenco, Z. Liu, M. Salmeron, *ChemCatChem* **2017**, *9*, 2318–2323.

[39] X. Frogneux, F. Borondics, S. Lefrançois, F. D'Accriscio, C. Sanchez, S. Carenco, *Catal. Sci. Technol.* **2018**, *8*, 5073–5080.

[40] A. Palazzolo, S. Carenco, *Chem. Mater.* **2021**, *33*, 7914–7922.

[41] R. F. André, L. Meyniel, S. Carenco, *Catal. Sci. Technol.* **2022**, *12*, 4572–4583.

[42] R. F. André, A. Palazzolo, C. Poucin, F. Ribot, S. Carenco, *Chempluschem* **2023**, *88*, DOI 10.1002/cplu.202300038.

[43] N. Fey, A. C. Tsipis, S. E. Harris, J. N. Harvey, A. G. Orpen, R. A. Mansson, *Chem. - A Eur. J.* **2006**, *12*, 291–302.

[44] J. Jover, J. Cirera, *Dalt. Trans.* **2019**, *48*, 15036–15048.

[45] M. G. Gasparyan, G. Ts.; Minasyan, G. G.; Torgomyan, A. M.; Ovakimyan, M. Zh.; Indzhikyan, *Armyanskii Khimicheskii Zhurnal* **1983**, *36*, 456–462.

[46] S. Carenco, S. Labouille, S. Bouchonnet, C. Boissière, X.-F. Le Goff, C. Sanchez, N. Mézailles, *Chem. - A Eur. J.* **2012**, *18*, 14165–14173.

[47] A. Pesesse, S. Carenco, *Catal. Sci. Technol.* **2021**, *11*, 5310–5320.

[48] H. Li, Q. Li, P. Wen, T. B. Williams, S. Adhikari, C. Dun, C. Lu, D. Itanze, L. Jiang, D. L. Carroll, G. L. Donati, P. M. Lundin, Y. Qiu, S. M. Geyer, *Adv. Mater.* **2018**, *30*,

DOI 10.1002/adma.201705796.

[49] J. L. Fiorio, N. López, L. M. Rossi, *ACS Catal.* **2017**, *7*, 2973–2980.

[50] E. Brunner, *J. Chem. Eng. Data* **1985**, *30*, 269–273.

[51] D.-H. Ha, L. M. Moreau, C. R. Bealing, H. Zhang, R. G. Hennig, R. D. Robinson, *J. Mater. Chem.* **2011**, *21*, 11498.

[52] H. Li, Q. Li, P. Wen, T. B. Williams, S. Adhikari, C. Dun, C. Lu, D. Itanze, L. Jiang, D. L. Carroll, G. L. Donati, P. M. Lundin, Y. Qiu, S. M. Geyer, *Adv. Mater.* **2018**, *30*, 1–8.

TOC Graphic

Catalytic amounts of phosphines, such as P^nBu_3 and PCy_3, have a positive effect on the activity of cobalt phosphide nano-urchins for the semi-hydrogenation of phenylacetylene at 100 °C under H_2 (7 bars).

@SophieCARENCO @lcmcp_paris